

Optimal SNR Analysis for Single-user RIS Systems

Ikram Singh*, Peter J. Smith†, Pawel A. Dmochowski*

*School of Engineering and Computer Science, Victoria University of Wellington, Wellington, New Zealand

†School of Mathematics and Statistics, Victoria University of Wellington, Wellington, New Zealand

email: {ikram.singh,peter.smith,pawel.dmochowski}@ecs.vuw.ac.nz

Abstract—In this paper, we present an analysis of the optimal uplink SNR of a SIMO Reconfigurable Intelligent Surface (RIS)-aided wireless link. We assume that the channel between base station and RIS is a rank-1 LOS channel while the user (UE)-RIS and UE-base station (BS) channels are correlated Rayleigh. We derive an exact closed form expression for the mean SNR and an approximation for the SNR variance leading to an accurate gamma approximation to the distribution of the UL SNR. Furthermore, we analytically characterise the effects of correlation on SNR, showing that correlation in the UE-BS channel can have negative effects on the mean SNR, while correlation in the UE-RIS channel improves system performance. For systems with a large number of RIS elements, correlation in the UE-RIS channel can cause an increase in the mean SNR of up to 27.32% relative to an uncorrelated channel.

I. INTRODUCTION

Reconfigurable Intelligent Surface (RIS) aided wireless networks are currently the subject of considerable research attention due to their ability to manipulate the channel between users (UEs) and base station (BS) via the RIS. Assuming that channel state information (CSI) is known at the RIS, one can intelligently alter the RIS phases, essentially changing the channel, to improve various aspects of system performance. Here, we focus on a single user system and assume the common system scenario where a RIS is carefully located near the BS such that a rank-1 line-of-sight (LOS) channel is formed between the BS and RIS.

System scenarios with a LOS channel between the BS-RIS and a single-user are also considered in [1]–[4] with motivation for the LOS assumption given in [3]. All of these existing works aim to enhance the system to achieve some optimal system performance (sum rate, SINR, etc.) by tuning the RIS phases. In particular, [3] gives a closed form RIS phase solution without the presence of a direct UE-BS channel for a single user setting, while [4] gives a closed form phase solution with the presence of a direct channel. However, once the optimal RIS has been defined there is no *exact* analysis of the mean SNR and no analysis of correlation impact on the mean SNR in [1]–[4].

For the UE to RIS and the direct UE to BS links, scattered channels are a reasonable assumption and spatial correlation in the channels is an important factor, especially at the RIS where small inter-element spacing may be envisaged. Several papers do consider spatial correlation in the small-scale fading channels [3], [5]–[11], however, these papers are simulation based and no analysis is given on the impact of correlation on the mean SNR.

Statistical properties of the channel have been investigated in existing literature. For example, [12], [13] provide a closed form expression for the mean SNR in the absence of a UE-BS channel with [13] additionally providing a probability density function (PDF) and a cumulative distribution function (CDF) for the distribution of the mean SNR. In [12], [14], an upper bound is given for the ergodic capacity and in [15] a lower bound is given for the ergodic capacity. However, there is no existing literature on closed form optimal expressions for the mean SNR and SNR variance for a RIS-aided wireless system, in the presence of correlated UE-BS, UE-RIS fading channels.

Hence, in this paper, we focus on an analysis of the optimal uplink (UL) SNR for a single user RIS aided link with a rank-1 LOS RIS-BS channel and correlated Rayleigh fading for the UE-BS and UE-RIS channels. In particular, for this system and channel model we make the following contributions:

- An exact closed-form result for mean SNR and an approximate closed form expression for SNR variance are derived. These are used to show that a gamma distribution provides a good approximation of the UL optimal SNR distribution.
- Exact closed-form expressions for both mean SNR and SNR variance are derived for uncorrelated Rayleigh channels and presented as a special case.
- The analysis is leveraged to gain insight into the impact of spatial correlation and system dimension on the mean SNR. We prove that correlation in the UE-BS channel can have negative effects, while correlation in the UE-RIS channel improves the mean SNR. For systems with a large number of RIS elements, the latter improvement saturates to a relative gain of approximately 27.32%.

Notation: $\mathbb{E}\{\cdot\}$ represents statistical expectation. $\Re\{\cdot\}$ is the Real operator. $\|\cdot\|_2$ denotes the ℓ_2 norm. Upper and lower boldface letters represent matrices and vectors, respectively. $\mathcal{CN}(\boldsymbol{\mu}, \mathbf{Q})$ denotes a complex Gaussian distribution with mean $\boldsymbol{\mu}$ and covariance matrix \mathbf{Q} . $\mathcal{U}[a, b]$ denotes a uniform random variable taking on values between a and b . χ_k^2 denotes a chi square distribution with k degrees of freedom. $\mathbf{1}_n$ represents an $n \times n$ matrix with unit entries. The transpose, Hermitian transpose and complex conjugate operators are denoted as $(\cdot)^T$, $(\cdot)^H$, $(\cdot)^*$, respectively. The trace and diagonal operators are denoted by $\text{tr}\{\cdot\}$ and $\text{diag}\{\cdot\}$, respectively. The angle of a vector \mathbf{x} of length N is defined as $\angle \mathbf{x} = [\angle x_1, \dots, \angle x_N]^T$ and the exponent of a vector is defined as $e^{\mathbf{x}} = [e^{x_1}, \dots, e^{x_N}]^T$. \otimes denotes the Kronecker

product.

II. SYSTEM MODEL

As shown in Fig. 1, we examine a RIS aided single user single input multiple output (SIMO) system where a RIS with N reflective elements is located close to a BS with M antennas such that a rank-1 LOS condition is achieved between the RIS and BS.

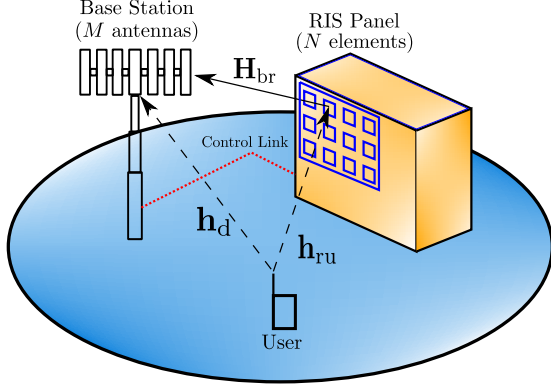


Fig. 1: System model where the red dashed line is the control link for the RIS phases.

A. Channel Model

Let $\mathbf{h}_d \in \mathbb{C}^{M \times 1}$, $\mathbf{h}_{ru} \in \mathbb{C}^{N \times 1}$, $\mathbf{H}_{br} \in \mathbb{C}^{M \times N}$ be the UE-BS, UE-RIS and RIS-BS channels, respectively. The diagonal matrix $\Phi \in \mathbb{C}^{N \times N}$, where $\Phi_{r,r} = e^{j\phi_r}$ for $r = 1, 2, \dots, N$, contains the reflection coefficients for each RIS element. The global UL channel is thus represented by

$$\mathbf{h} = \mathbf{h}_d + \mathbf{H}_{br} \Phi \mathbf{h}_{ru}. \quad (1)$$

In the channel model, we consider the correlated Rayleigh channels: $\mathbf{h}_d = \sqrt{\beta_d} \mathbf{R}_d^{1/2} \mathbf{u}_d$ and $\mathbf{h}_{ru} = \sqrt{\beta_{ru}} \mathbf{R}_{ru}^{1/2} \mathbf{u}_{ru} \triangleq \sqrt{\beta_{ru}} \tilde{\mathbf{h}}_{ru}$ where β_d and β_{ru} are the link gains, \mathbf{R}_d , \mathbf{R}_{ru} are the correlation matrices for UE-BS and UE-RIS links respectively and \mathbf{u}_d , $\mathbf{u}_{ru} \sim \mathcal{CN}(\mathbf{0}, \mathbf{I})$. The rank-1 LOS channel from RIS to BS has link gain β_{br} and is given by $\mathbf{H}_{br} = \sqrt{\beta_{br}} \mathbf{a}_b \mathbf{a}_r^H$ where \mathbf{a}_b and \mathbf{a}_r are topology specific steering vectors at the BS and RIS respectively. Particular examples of steering vectors for a vertical uniform rectangular array (VURA) are defined in Sec. V.

The correlation matrices are assumed to follow the well-known exponential decay model,

$$(\mathbf{R}_{ru})_{ik} = \rho_{ru}^{\frac{d_{i,k}}{d_b}}, \quad (\mathbf{R}_d)_{ik} = \rho_d^{\frac{d_{i,k}}{d_r}} \quad (2)$$

where $0 < \rho_{ru} < 1$, $0 < \rho_d < 1$. $d_{i,k}$ is the distance between the i^{th} and k^{th} antenna/element at the BS/RIS. d_b and d_r are the nearest-neighbour BS antenna separation and RIS element separation, respectively, which are measured in wavelength units. ρ_d and ρ_{ru} are the nearest neighbour BS antenna and RIS element correlations, respectively.

B. Optimal SNR

Using (1), the received signal at the BS is,

$$\mathbf{r} = (\mathbf{h}_d + \mathbf{H}_{br} \Phi \mathbf{h}_{ru}) s + \mathbf{n} = \mathbf{h} s + \mathbf{n}, \quad (3)$$

where s is the transmitted signal with power E_s and $\mathbf{n} \sim \mathcal{CN}(\mathbf{0}, \sigma^2 \mathbf{I})$. For a single user system, matched filtering (MF) is the optimal combining method, with UL SNR, given by

$$\text{SNR} = \mathbf{h}^H \bar{\tau}, \quad (4)$$

where $\bar{\tau} = \frac{E_s}{\sigma^2}$. The optimal RIS phase matrix to maximize (4) can be computed using the main steps outlined in [4, Sec. III-B] but using an UL channel model instead of downlink. Substituting the channel vectors and through some algebraic manipulation, the optimal RIS phase matrix is

$$\Phi = \frac{\mathbf{a}_b^H \mathbf{h}_d}{|\mathbf{a}_b^H \mathbf{h}_d|} \text{diag}\{e^{j\angle \mathbf{a}_r}\} \text{diag}\{e^{-j\angle \mathbf{h}_{ru}}\}. \quad (5)$$

Substituting (5) into \mathbf{h} , the optimal UL global channel is,

$$\mathbf{h} = \mathbf{h}_d + \sqrt{\beta_{br} \beta_{ru}} \psi \sum_{n=1}^N \left| \tilde{\mathbf{h}}_{ru,n} \right| \mathbf{a}_b, \quad (6)$$

where $\psi = \frac{\mathbf{a}_b^H \mathbf{h}_d}{|\mathbf{a}_b^H \mathbf{h}_d|}$. Hence, the optimal UL SNR is

$$\text{SNR} = (\mathbf{h}_d^H + \alpha^* \mathbf{a}_b^H) (\mathbf{h}_d + \alpha \mathbf{a}_b) \bar{\tau}, \quad (7)$$

where $\alpha = \sqrt{\beta_{br} \beta_{ru}} \psi \sum_{n=1}^N \left| \tilde{\mathbf{h}}_{ru,n} \right| \triangleq \sqrt{\beta_{br} \beta_{ru}} \psi Y$.

III. $\mathbb{E}\{\text{SNR}\}$ AND $\text{VAR}\{\text{SNR}\}$

A. Correlated Rayleigh Case

Here, we provide an exact closed form result for $\mathbb{E}\{\text{SNR}\}$ and an exact expression for $\text{Var}\{\text{SNR}\}$.

Theorem 1. *The mean SNR is given by*

$$\mathbb{E}\{\text{SNR}\} = \left(\beta_d M + \frac{N A \pi \sqrt{\beta_d \beta_{br} \beta_{ru}}}{2} + \beta_{br} \beta_{ru} M(N+F) \right) \bar{\tau}, \quad (8)$$

with F given by

$$F = \sum_{i=1}^N \sum_{\substack{j=1 \\ i \neq j}}^N \frac{\pi}{4} (1 - |\rho_{ij}|^2)^2 {}_2F_1 \left(\frac{3}{2}, \frac{3}{2}; 1; |\rho_{ij}|^2 \right), \quad (9)$$

and $A = \left\| \mathbf{R}_d^{1/2} \mathbf{a}_b \right\|_2$, where ${}_2F_1(\cdot)$ is the Gaussian hypergeometric function and $\rho_{ij} = (\mathbf{R}_{ru})_{ij}$.

Proof. See Appendix A for the derivation of (8). ■

Theorem 2. *The SNR variance is given by*

$$\begin{aligned} \text{Var}\{\text{SNR}\} &= \left(\beta_d^2 \text{tr}\{\mathbf{R}_d^2\} + \beta_d^{3/2} \sqrt{\beta_{br} \beta_{ru}} N \pi (B - MA) \right. \\ &\quad + \beta_d \beta_{br} \beta_{ru} A^2 \left(4(N+F) - \frac{N^2 \pi^2}{4} \right) \\ &\quad + MA \sqrt{\beta_d} (\beta_{br} \beta_{ru})^{3/2} (2\sqrt{\pi} C_1 - N(N+F)\pi) \\ &\quad \left. + (M \beta_{br} \beta_{ru})^2 (C_2 - (N+F)^2) \right) \bar{\tau}^2, \quad (10) \end{aligned}$$

where $B = MA + \mathbf{a}_b^H \mathbf{R}_d^2 \mathbf{a}_b / 2A$, F is given by (9), A is given in Theorem 1 and $C_1 = \mathbb{E}\{Y^3\}$, $C_2 = \mathbb{E}\{Y^4\}$.

Proof. See Appendix B for the derivation of (10). ■

In (10), all terms are known except for C_1 and C_2 , the third and fourth moments of Y . To the best of our knowledge, these moments are intractable so we present approximations of C_1 and C_2 in the following Corollary.

Corollary. *To obtain an approximation of the SNR variance in closed form, we approximate the 3rd and 4th moments of Y by,*

$$\mathbb{E}\{Y^3\} = b^3 a \prod_{k=1}^2 (k+a), \quad \mathbb{E}\{Y^4\} = b^4 a \prod_{k=1}^3 (k+a) \quad (11)$$

with

$$a = \frac{N^2 \pi}{4(N+F) - N^2 \pi}, \quad b = \frac{2}{N\sqrt{\pi}} \left(N + F - \frac{N^2 \pi}{4} \right).$$

where F is given by (9).

Proof. See Appendix C for the derivation of (11). ■

From Theorem 1 and the Corollary, we have $\mathbb{E}\{\text{SNR}\}$ and an approximation to $\text{Var}\{\text{SNR}\}$. This enable us to fit a gamma distribution as an approximation to the SNR distribution. Motivation and reasoning for this approach is given in Sec. V-A.

B. Special Case: Uncorrelated Rayleigh Case

For independent Rayleigh fading, we provide exact closed form expressions for both $\mathbb{E}\{\text{SNR}\}$ and $\text{Var}\{\text{SNR}\}$. Here, $\mathbf{h}_d, \mathbf{h}_{ru} \sim \mathcal{CN}(\mathbf{0}, \mathbf{I})$ (i.e. $\mathbf{R}_d = \mathbf{I}_M$ and $\mathbf{R}_{ru} = \mathbf{I}_N$). As such, (9) simplifies to

$$F_u = \sum_{i=1}^N \sum_{\substack{j=1 \\ i \neq j}}^N \frac{\pi}{4} = N(N-1) \frac{\pi}{4}. \quad (12)$$

From $\|\mathbf{a}_b\|_2 = \sqrt{M}$, the value of $\mathbb{E}\{\text{SNR}\}$ for uncorrelated channels is,

$$\left(\beta_d M + \frac{\sqrt{M} N \pi}{2} \sqrt{\beta_d \beta_{br} \beta_{ru}} + \beta_{br} \beta_{ru} M (N + F_u) \right) \bar{\tau}. \quad (13)$$

Using (12) and since $\mathbf{R}_d = \mathbf{I}_M$ and $\mathbf{R}_{ru} = \mathbf{I}_N$, an exact expression for $\text{Var}\{\text{SNR}\}$ is given by

$$\begin{aligned} & \left(\beta_d^2 M + \beta_d^{3/2} \sqrt{\beta_{br} \beta_{ru}} N \pi (B_u - 2M^{3/2}) \right. \\ & + \beta_d \beta_{br} \beta_{ru} M \left(4(N + F_u) - \frac{N^2 \pi^2}{4} \right) \\ & + M^{3/2} \sqrt{\beta_d} (\beta_{br} \beta_{ru})^{3/2} (2\sqrt{\pi} C_{u1} - N(N + F_u) \pi) \\ & \left. + (M \beta_{br} \beta_{ru})^2 (C_{u2} - (N + F_u)^2) \right) \bar{\tau}^2, \quad (14) \end{aligned}$$

with

$$\begin{aligned} B_u &= M^{3/2} + \frac{1}{2} \sqrt{M} \\ C_{u1} &= \frac{N\sqrt{\pi}}{2} \left(\frac{\pi}{4} \prod_{k=1}^2 (N-k) + 3N - \frac{3}{2} \right) \\ C_{u2} &= 2N + \binom{N}{2} \left(\prod_{k=2}^3 (N-k) \frac{\pi^2}{8} + 6 + 3\pi(N-1) \right) \end{aligned}$$

where F_u is given by (12). Derivations for C_{u1} , C_{u2} are omitted for reasons of space, but can be easily obtained by expanding Y^3 , Y^4 and computing the expectation of each term using the following: $\mathbb{E}\left\{ \left| \tilde{\mathbf{h}}_{ru,i} \right|^4 \right\} = 2$, $\mathbb{E}\left\{ \left| \tilde{\mathbf{h}}_{ru,i} \right|^3 \right\} = 3\sqrt{\pi}/4$, $\mathbb{E}\left\{ \left| \tilde{\mathbf{h}}_{ru,i} \right|^2 \right\} = 1$, $\mathbb{E}\left\{ \left| \tilde{\mathbf{h}}_{ru,i} \right| \right\} = \sqrt{\pi}/2$.

IV. PERFORMANCE INSIGHTS BASED ON $\mathbb{E}\{\text{SNR}\}$

Correlation in channels \mathbf{h}_d and \mathbf{h}_{ru} have seperable effects on the mean SNR in (8). Specifically, the second term in (8) is only affected by ρ_d and the third term is only affected by ρ_{ru} whilst the first term is affect by neither. Here, we present an analysis of $\mathbb{E}\{\text{SNR}\}$ with respect to the correlation levels ρ_{ru}, ρ_d and give asymptotic results for large numbers of RIS elements (large N).

A. Effect of ρ_{ru} on $\mathbb{E}\{\text{SNR}\}$

With respect to the correlation level ρ_{ru} , (8) can be lower and upper bounded due to F being monotonic in ρ_{ru} [16, Eq. (15.1.1)]. The upper bound for (9) as $\rho_{ru} \rightarrow 1$ is

$$F_{\text{UB}} \stackrel{(a)}{=} \sum_{i=1}^N \sum_{\substack{j=1 \\ i \neq j}}^N \frac{\pi}{4} {}_2F_1 \left(-\frac{1}{2}, -\frac{1}{2}; 1; 1 \right) \stackrel{(b)}{=} N(N-1), \quad (15)$$

where (a) uses [16, Eq. (15.3.3)] to perform a linear transformation of the hypergeometric function and (b) uses [16, Eq. (15.1.20)] to reduce the hypergeometric function to a known value along with evaluation of the double summation. Using (12) and (15), (9) has the following upper and lower bounds,

$$F_u = N(N-1) \frac{\pi}{4} \leq F \leq N(N-1). \quad (16)$$

This means that the upper and lower bounds for SNR with respect to ρ_{ru} are

$$\mathbb{E}\{\text{SNR}\}_{\text{UB}} = \left(\beta_d M + \frac{NA\pi}{2} \sqrt{\beta_d \beta_{br} \beta_{ru}} + \beta_{br} \beta_{ru} M N^2 \right) \bar{\tau}, \quad (17)$$

$$\mathbb{E}\{\text{SNR}\}_{\text{LB}} = \left(\beta_d M + \frac{NA\pi}{2} \sqrt{\beta_d \beta_{br} \beta_{ru}} + \beta_{br} \beta_{ru} M (N + F_u) \right) \bar{\tau}. \quad (18)$$

Hence, correlation in \mathbf{h}_{ru} improves the mean SNR. From (17) and (18) we observe that the first term in $\mathbb{E}\{\text{SNR}\}$ is of order M and the third term is of order MN^2 . In Sec. IV-B we show that the second term has a maximum order of MN . Hence, the third term is dominant giving $\mathbb{E}\{\text{SNR}\} = \mathcal{O}(MN^2)$ and

the largest channel effect will be an increase in SNR due to correlation at the RIS.

B. Effect of ρ_d on $\mathbb{E}\{\text{SNR}\}$

The only variable in (8) that is affected by ρ_d is A . As $\rho_d \rightarrow 0$, $A \rightarrow \sqrt{M}$. As $\rho_d \rightarrow 1$, $\mathbf{R}_d \rightarrow \mathbf{1}_M$ which means that

$$A = \left\| \mathbf{R}_d^{1/2} \mathbf{a}_b \right\|_2 \rightarrow \frac{1}{\sqrt{M}} \left\| \mathbf{1}_M \mathbf{a}_b \right\|_2 = \left| \sum_{i=1}^M \mathbf{a}_{b,i} \right| \leq M.$$

Hence, the second term in (8) has a maximum order of MN as stated above. Although the maximum order can be achieved with perfect correlation ($\rho_d = 1$), for typical environments the value of A tends to reduce as correlation is increased. To explain this property we show via an example based on a uniform linear array (ULA) that for highly correlated BS antennas, \sqrt{M} tends to be larger than $\left| \sum_{i=1}^M \mathbf{a}_{b,i} \right|$ for large M . For a ULA, ignoring elevation angles, the steering vector elements can be given by $\mathbf{a}_{b,i} = e^{j2\pi(i-1)d_b \sin(\theta)}$ where θ is the azimuth angle of arrival at the BS. Here,

$$\left| \sum_{i=1}^M \mathbf{a}_{b,i} \right| = \left| \frac{1 - e^{j2M\pi d_b \sin(\theta)}}{1 - e^{j2\pi d_b \sin(\theta)}} \right| = \left| \frac{\sin(M\pi d_b \sin(\theta))}{\sin(\pi d_b \sin(\theta))} \right|.$$

This well-known sinusoidal ratio is much smaller than \sqrt{M} for large M as long as θ is not arbitrarily close to zero. Therefore, systems with a large number of BS antennas can expect greater system performance when \mathbf{h}_d is uncorrelated unless the RIS-BS link is extremely close to broadside.

In summary, high correlation at the RIS and low correlation at the BS tend to be beneficial. We refer to this scenario as the *favorable channel scenario*.

C. Favorable Channel Scenario and Asymptotic Analysis

Using the analysis in Sec. IV-A and Sec. IV-B, the favorable channel scenario is given by: $\mathbf{h}_{ru} \sim \mathcal{CN}(\mathbf{0}, \mathbf{1}_M)$, $\mathbf{h}_d \sim \mathcal{CN}(\mathbf{0}, \mathbf{I}_N)$. The resulting mean SNR is obtained by substituting the UB of (16) and $A = \sqrt{M}$ into (8). This gives the very simple result

$$\mathbb{E}\{\text{SNR}_{\text{fav}}\} = \left(\beta_d M + \frac{N\sqrt{M}\pi}{2} \sqrt{\beta_d \beta_{br} \beta_{ru}} + \beta_{br} \beta_{ru} MN^2 \right) \bar{\tau}. \quad (19)$$

Next, we consider the asymptotic gains achievable through increased correlation at the RIS. The relative gain due to correlation can be defined as

$$\text{Gain}_{\text{corr}} = \frac{\mathbb{E}\{\text{SNR}\}_{\text{UB}} - \mathbb{E}\{\text{SNR}\}_{\text{LB}}}{\mathbb{E}\{\text{SNR}\}_{\text{LB}}} \stackrel{(a)}{=} \frac{(4 - \pi)N^2 + (\pi - 4)N}{\pi N^2 + (4 - \pi)N + \frac{4\beta_d}{\beta_{br}\beta_{ru}} + \frac{2NA\pi\sqrt{\beta_d}}{M\sqrt{(\beta_{br}\beta_{ru})}}} \quad (20)$$

where (a) involves substituting (17) and (18) and performing simple algebraic manipulations. Therefore, as $N \rightarrow \infty$,

$$\text{Gain}_{\text{max}} = \lim_{N \rightarrow \infty} \text{Gain}_{\text{corr}} = \frac{4 - \pi}{\pi} \approx 27.32\%.$$

Hence, for a large RIS, the maximum gain due to correlation in the UE-RIS Rayleigh channel is approximately 27.32%.

V. RESULTS

Here, we present numerical results to verify the analysis in Secs. III and IV. In this paper we do not consider any cell-wide averaging as the focus is on the SNR distribution over the fast fading for fixed link gains. Furthermore, the relationship between the SNR and the gains, β_d , β_{br} and β_{ru} , is straightforward as shown in (8). Hence, we present numerical results for fixed link gains. In particular, as the RIS-BS link is LOS we assume $\beta_d = d_{br}^{-2}$ where $d_{br} = 20\text{m}$. Next, for simplicity, we select a common value for β_d and β_{ru} given by $\beta_d = \beta_{ru} = 0.59$. This was chosen to give the 95%-ile of the SNR distribution as 25 dB in the baseline case of moderate channel correlation (see Fig 2, the $\rho_d = \rho_{ru} = 0.7$ scenario), with $M = 32$, $N = 64$.

As stated in Sec. II-A, the steering vectors for \mathbf{H}_{br} are not restricted to any particular formation. However, for simulation purposes, we will use the VURA model as outlined in [17], but in the $y - z$ plane with equal spacing in both dimensions at both the RIS and BS. The y, z components of the steering vector at the BS are $\mathbf{a}_{b,y}$ and $\mathbf{a}_{b,z}$ which are given by

$$\begin{aligned} & [1, e^{j2\pi d_b \sin(\theta_A) \sin(\omega_A)}, \dots, e^{j2\pi d_b (M_x - 1) \sin(\theta_A) \sin(\omega_A)}]^T, \\ & [1, e^{j2\pi d_b \cos(\theta_A)}, \dots, e^{j2\pi d_b (M_z - 1) \cos(\theta_A)}]^T, \end{aligned}$$

respectively. Similarly at the RIS, $\mathbf{a}_{r,y}$ and $\mathbf{a}_{r,z}$ are defined by,

$$\begin{aligned} & [1, e^{j2\pi d_r \sin(\theta_D) \sin(\omega_D)}, \dots, e^{j2\pi d_r (N_x - 1) \sin(\theta_D) \sin(\omega_D)}]^T, \\ & [1, e^{j2\pi d_r \cos(\theta_D)}, \dots, e^{j2\pi d_r (N_z - 1) \cos(\theta_D)}]^T, \end{aligned}$$

respectively where $M = M_x M_z$, $N = N_x N_z$, $d_b = 0.5$, $d_r = 0.2$, where d_b and d_r are in wavelength units. Therefore, the steering vectors at the BS and RIS are then given by,

$$\mathbf{a}_b = \mathbf{a}_{b,y} \otimes \mathbf{a}_{b,z} \quad , \quad \mathbf{a}_r = \mathbf{a}_{r,y} \otimes \mathbf{a}_{r,z}, \quad (21)$$

respectively, where θ_A and ω_A are elevation/azimuth angles of arrival (AOAs) at the BS and θ_D, ω_D are the corresponding angles of departure (AODs) at the RIS. The elevation/azimuth angles are selected based on the following geometry representing a range of LOS \mathbf{H}_{br} links with less elevation variation than azimuth variation: $\theta_D \sim \mathcal{U}[70^\circ, 90^\circ]$, $\omega_D \sim \mathcal{U}[-30^\circ, 30^\circ]$, $\theta_A = 180^\circ - \theta_D$, $\omega_A \sim \mathcal{U}[-30^\circ, 30^\circ]$. For all results in this paper we use a single sample from this range of angles given by $\theta_D = 77.1^\circ, \omega_D = 19.95^\circ, \theta_A = 109.9^\circ, \omega_A = -29.9^\circ$. Note that all of these parameter values and variable definitions are not altered throughout the results and figures, unless specified otherwise.

A. Approximate CDF for SNR

It is known that the SNR of a wide range of fading channels can be approximately modeled by a mixture gamma distribution [18]. Also, it is well-known that a single gamma approximation is often reasonable for a variable which is the sum of a number of positive random variables, see [12] for

example. Motivated by this, we approximate the SNR in (7) by a single gamma variable.

The shape parameter of a gamma approximation to the SNR is given by $k_\gamma = \frac{\mathbb{E}\{\text{SNR}\}^2}{\text{Var}\{\text{SNR}\}}$ and the scale parameter is $\theta_\gamma = \frac{\text{Var}\{\text{SNR}\}}{\mathbb{E}\{\text{SNR}\}}$ where $\mathbb{E}\{\text{SNR}\}$ and $\text{Var}\{\text{SNR}\}$ are given in Sec. III. Using these values of k_γ, θ_γ , the analytical and simulated SNR CDFs are shown in Fig. 2 for $N = 64$ and $N = 256$, both with $\rho_{\text{ru}} = \rho_{\text{d}} = \{0, 0.7, 0.95\}$. When computing the analytical SNR CDFs, for $\rho_{\text{ru}} = \rho_{\text{d}} = 0$, (13) and (14) were used and for $\rho_{\text{ru}} = \rho_{\text{d}} \neq 0$, (8) and (10) were used. As expected, there is a very good agreement between the

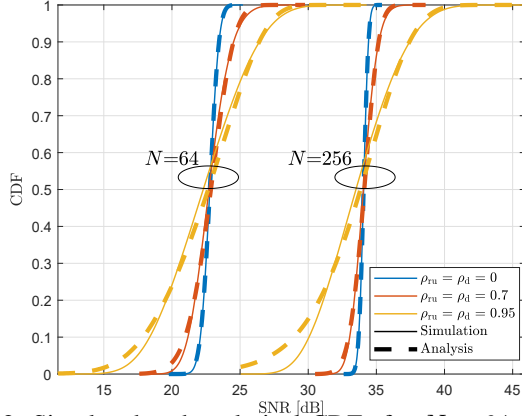


Fig. 2: Simulated and analytical CDFs for $N = 64$ and $N = 256$, both with $\rho_{\text{ru}} = \rho_{\text{d}} = \{0, 0.7, 0.95\}$

simulated and analytical SNR CDFs when $\rho_{\text{d}} = \rho_{\text{d}} = 0$ due to exact mean SNR and SNR variance expressions. Increasing the correlation level, causes the CDF agreement to deviate slightly in the low SNR region, especially in the highest correlation scenario. However, good agreement is maintained in the mid-high SNR region. The gamma distribution therefore provides a good representation of the UL SNR unless the correlations become very high.

B. $\rho_{\text{d}}, \rho_{\text{ru}}$ and Asymptotic Analysis Results

Here, we verify the performance insights based on $\mathbb{E}\{\text{SNR}\}$. Fig. 3 represents SNR simulations and analysis for three different correlation scenarios: $\rho_{\text{ru}} = \rho_{\text{d}} = 0$, $\rho_{\text{ru}} = \rho_{\text{d}} = 1$ and the favorable channel scenario $\rho_{\text{ru}} = 1, \rho_{\text{d}} = 0$. The left subfigure in Fig. 3 shows the quadratic increase in mean SNR, as predicted by the analysis. The favorable channel scenario yields the highest mean SNR but the increase over perfect correlation in both channels is marginal. The lowest SNR occurs when both channels are uncorrelated. Fig. 3 also shows that for all correlation level scenarios, the theoretical analysis agrees with the simulation.

The right subfigure in Fig. 3 shows the accuracy of the SNR variance approximation. There is a perfect agreement for the case where \mathbf{h}_{ru} and \mathbf{h}_{d} are uncorrelated. In the correlated cases, the analysis and simulation agree closely for low N but begin to deviate slightly as N grows. This is also reflected in Fig. 2 as the CDF agreement between simulation and analysis is worse for $N = 256$ compared to $N = 64$ as

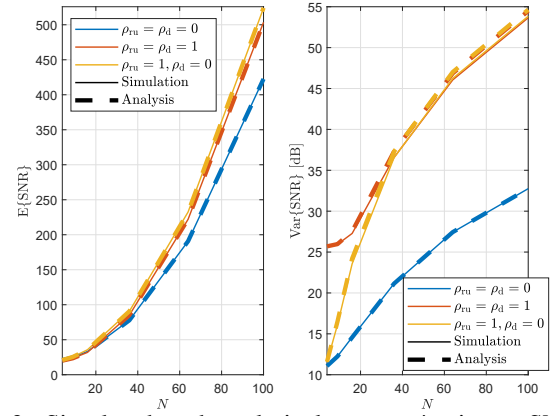


Fig. 3: Simulated and analytical average/variace SNR for three different correlated level scenarios: $\rho_{\text{ru}} = \rho_{\text{d}} = 0$, $\rho_{\text{ru}} = \rho_{\text{d}} = 1$ and favorable channel scenario $\rho_{\text{ru}} = 1, \rho_{\text{d}} = 0$.

$\rho_{\text{d}}, \rho_{\text{ru}} \rightarrow 1$. Note that the analytical CDFs show a longer lower tail, partially caused by the over-estimate of the variance. As N grows, observe that the variance for scenarios $\rho_{\text{ru}} = \rho_{\text{d}} = 1$ and $\rho_{\text{ru}} = 1, \rho_{\text{d}} = 0$ converge to approximately the same value. This is because the effects of correlation in \mathbf{h}_{d} are reduced by large N .

Finally, in Fig. 4 we verify the mean SNR relative gain due to correlation in \mathbf{h}_{ru} , and verify the asymptotic analysis in Sec. IV-A and Sec. IV-C. For simplicity, we assume all three channels have the same link gain and let $\beta_{\text{d}} = \beta_{\text{ru}} = \beta_{\text{br}} = 1$. Fig. 4 verifies the analysis in Sec. IV-C demonstrating an

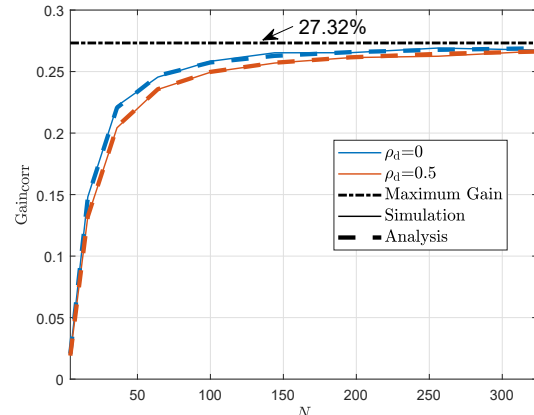


Fig. 4: Average SNR gain due to correlation in \mathbf{h}_{ru} for varying RIS sizes and correlation in \mathbf{h}_{d} .

increasing gain with correlation saturating at approximately 27.32%. Introducing correlation in the direct channel causes the gain to be lower. However, as explained in the analysis, for large RIS elements, this negative effect is reduced.

VI. CONCLUSION

In this paper, we derive an exact closed form expression for the mean SNR of the optimal single user RIS design where spatially correlated Rayleigh fading is assumed for the UE-BS and UE-RIS channels and the RIS-BS channel is LOS. We also provide an accurate approximation to the SNR variance and a gamma approximation to the CDF of the SNR. The

results offers new insight into how spatial correlation impacts the mean SNR and scenarios in which we would expect high SNR performance.

APPENDIX A
 $\mathbb{E}\{\text{SNR}\}$ DERIVATION IN SEC. III-A

Substituting the channel vectors and matrices described in Sec. II-A into (7) gives

$$\text{SNR} = \left(\beta_d \mathbf{u}_d^H \mathbf{R}_d \mathbf{u}_d + 2\sqrt{\beta_d} \Re \left\{ \alpha \mathbf{u}_d^H \mathbf{R}_d^{1/2} \mathbf{a}_b \right\} + |\alpha|^2 M \right) \bar{\tau} \\ \triangleq (S_1 + S_2 + S_3) \bar{\tau}.$$

We now compute $\mathbb{E}\{\text{SNR}\}$ by taking the expectation of each individual term in the above expression.

Term 1: Since $\mathbf{u}_d \sim \mathcal{CN}(\mathbf{0}, \mathbf{I})$,

$$\mathbb{E}\{S_1\} = \beta_d \text{tr}\{\mathbf{R}_d\} = \beta_d M. \quad (22)$$

Term 2: Substituting α from Sec. II-B we have,

$$\mathbb{E}\{S_2\} = 2\sqrt{\beta_d \beta_{br} \beta_{ru}} \mathbb{E} \left\{ \sum_{n=1}^N |\tilde{\mathbf{h}}_{ru,n}| \right\} \mathbb{E} \left\{ \left| \mathbf{a}_b^H \mathbf{R}_d^{1/2} \mathbf{u}_d \right| \right\} \\ = 2\sqrt{\beta_d \beta_{br} \beta_{ru}} \mathbb{E}\{Y\} \mathbb{E} \left\{ \left| \mathbf{a}_b^H \mathbf{R}_d^{1/2} \mathbf{u}_d \right| \right\}.$$

Since $\mathbf{h}_{ru} \sim \mathcal{CN}(\mathbf{0}, \mathbf{R}_{ru})$ it follows that $\mathbb{E}\{Y\} = \frac{N\sqrt{\pi}}{2}$ [19].

To compute $\mathbb{E} \left\{ \left| \mathbf{a}_b^H \mathbf{R}_d^{1/2} \mathbf{u}_d \right| \right\}$, note the following results. As $\mathbf{u}_d \sim \mathcal{CN}(\mathbf{0}, \mathbf{I}_M)$, it follows that $\mathbf{a}_b^H \mathbf{R}_d^{1/2} \mathbf{u}_d$ is zero mean complex Gaussian with

$$\mathbb{E} \left\{ \left| \mathbf{a}_b^H \mathbf{R}_d^{1/2} \mathbf{u}_d \right|^2 \right\} = \left\| \mathbf{R}_d^{1/2} \mathbf{a}_b \right\|_2^2.$$

As such, we have $\left| \mathbf{a}_b^H \mathbf{R}_d^{1/2} \mathbf{u}_d \right| \sim \frac{1}{\sqrt{2}} \left\| \mathbf{R}_d^{1/2} \mathbf{a}_b \right\|_2 X^{1/2}$ where $X \sim \chi_2^2$ is a central chi-squared variable. By the moments of a central chi-square distribution with 2 degrees of freedom,

$$\mathbb{E} \left\{ \left| \mathbf{a}_b^H \mathbf{R}_d^{1/2} \mathbf{u}_d \right| \right\} = \left\| \mathbf{R}_d^{1/2} \mathbf{a}_b \right\|_2 \frac{\sqrt{\pi}}{2}. \quad (23)$$

Hence,

$$\mathbb{E}\{S_2\} = \frac{NA\pi}{2} \sqrt{\beta_d \beta_{br} \beta_{ru}}, \quad (24)$$

where $A = \left\| \mathbf{R}_d^{1/2} \mathbf{a}_b \right\|_2$.

Term 3: Using $|\psi| = 1$ (where ψ is given in Sec. II-B) we have $S_3 = M\beta_{br}\beta_{ru}Y^2$ and expanding Y gives

$$\mathbb{E}\{Y^2\} = \sum_{i=1}^N \mathbb{E} \left\{ \left| \tilde{\mathbf{h}}_{ru,i} \right|^2 \right\} + \sum_{i=1}^N \sum_{\substack{j=1 \\ i \neq j}}^N \mathbb{E} \left\{ \left| \tilde{\mathbf{h}}_{ru,i} \right| \left| \tilde{\mathbf{h}}_{ru,j} \right| \right\}.$$

Using [19, Eq. (16)], each individual expectation in the double summation is,

$$\mathbb{E} \left\{ \left| \tilde{\mathbf{h}}_{ru,i} \right| \left| \tilde{\mathbf{h}}_{ru,j} \right| \right\} = \frac{\pi}{4} \left(1 - |\rho_{ij}|^2 \right)^2 {}_2F_1 \left(\frac{3}{2}, \frac{3}{2}; 1; |\rho_{ij}|^2 \right),$$

where ${}_2F_1(\cdot)$ is the Gaussian hypergeometric function and $\rho_{ij} = (\mathbf{R}_{ru})_{ij}$. Using this, we have $\mathbb{E}\{Y^2\} = N + F$, where F is given by (9), giving the final result

$$\mathbb{E}\{S_3\} = \beta_{br}\beta_{ru}M(N + F). \quad (25)$$

Combining (22), (24) and (25) completes the derivation.

APPENDIX B
 $\text{VAR}\{\text{SNR}\}$ DERIVATION IN SEC. III-A

To compute the variance we take the square of (7) giving,

$$\text{SNR}^2 = \left(\beta_d^2 (\mathbf{u}_d^H \mathbf{R}_d \mathbf{u}_d)^2 + 4\beta_d^{3/2} \mathbf{u}_d^H \mathbf{R}_d \mathbf{u}_d \Re \left\{ \alpha \mathbf{u}_d^H \mathbf{R}_d^{1/2} \mathbf{a}_b \right\} \right. \\ \left. + 2\beta_d M |\alpha|^2 \mathbf{u}_d^H \mathbf{R}_d \mathbf{u}_d + 4\beta_d \Re \left\{ \alpha \mathbf{u}_d^H \mathbf{R}_d^{1/2} \mathbf{a}_b \right\}^2 \right. \\ \left. + 4\sqrt{\beta_d} M |\alpha|^2 \Re \left\{ \alpha \mathbf{u}_d^H \mathbf{R}_d^{1/2} \mathbf{a}_b \right\} + |\alpha|^4 M^2 \right) \bar{\tau}^2 \\ \triangleq (T_1 + T_2 + T_3 + T_4 + T_5 + T_6) \bar{\tau}^2. \quad (26)$$

Obtaining $\mathbb{E}\{\text{SNR}^2\}$ is done by performing the expectation of each term in (26).

Term 1: Using [20, Eq. (9)] and $\mathbf{u}_d \sim \mathcal{CN}(\mathbf{0}, \mathbf{I})$,

$$\mathbb{E}\{T_1\} = \beta_d^2 (\text{tr}\{\mathbf{R}_d^2\} + M^2). \quad (27)$$

Term 2: Expanding the second term gives,

$$\mathbb{E}\{T_2\} = 4\beta_d^{3/2} \sqrt{\beta_{br}\beta_{ru}} Y \mathbf{u}_d^H \mathbf{R}_d \mathbf{u}_d \left| \mathbf{u}_d^H \mathbf{R}_d^{1/2} \mathbf{a}_b \right|, \quad (28)$$

where Y is defined in Sec. II-B. To find the expectation of (28), we introduce the following variables: Let \mathbf{P} be any orthonormal matrix with first column equal to $\mathbf{p}_1 = \mathbf{R}_d^{1/2} \mathbf{a}_b \left\| \mathbf{R}_d^{1/2} \mathbf{a}_b \right\|_2^{-1}$. Also let $\mathbf{x} = \mathbf{P}^H \mathbf{u}_d \sim \mathcal{CN}(\mathbf{0}, \mathbf{I})$ and $\mathbf{Q} = \mathbf{P}^H \mathbf{R}_d \mathbf{P}$, then the random component of (28), neglecting Y , can be rewritten as,

$$\mathbf{u}_d^H \mathbf{R}_d \mathbf{u}_d \left| \mathbf{u}_d^H \mathbf{R}_d^{1/2} \mathbf{a}_b \right| = \mathbf{x}^H \mathbf{Q} \mathbf{x} \left| \mathbf{x}^H \mathbf{P} \mathbf{p}_1 \right| \left\| \mathbf{R}_d^{1/2} \mathbf{a}_b \right\|_2 \\ = \mathbf{x}^H \mathbf{Q} \mathbf{x} |x_1| \left\| \mathbf{R}_d^{1/2} \mathbf{a}_b \right\|_2, \quad (29)$$

since $\mathbf{P}^H \mathbf{p}_1 = [1, \mathbf{0}_{M-1}]^T$. Note that,

$$\mathbb{E} \left\{ \mathbf{x}^H \mathbf{Q} \mathbf{x} |x_1| \right\} = \mathbb{E} \left\{ \sum_{i=1}^M \sum_{j=1}^M \mathbf{Q}_{ij} x_i^* x_j |x_1| \right\} \\ = \mathbf{Q}_{11} \mathbb{E} \left\{ |x_1|^3 \right\} + (\text{tr}\{\mathbf{Q}\} - \mathbf{Q}_{11}) \mathbb{E} \left\{ |x_1| \right\} \\ = \frac{\sqrt{\pi} \mathbf{a}_b^H \mathbf{R}_d^2 \mathbf{a}_b}{4A^2} + M \frac{\sqrt{\pi}}{2}$$

since $\mathbb{E}\{|x_1|\} = \sqrt{\pi}/2$, $\mathbb{E}\{|x_1|^3\} = 3\sqrt{\pi}/4$, $\text{tr}\{\mathbf{Q}\} = \text{tr}\{\mathbf{R}_d\} = M$ and $\mathbf{Q}_{11} = \mathbf{p}_1^H \mathbf{R}_d \mathbf{p}_1 = \frac{\mathbf{a}_b^H \mathbf{R}_d^2 \mathbf{a}_b}{\mathbf{a}_b^H \mathbf{R}_d \mathbf{a}_b}$ and A is defined in Appendix A. Using the above result and the result for $\mathbb{E}\{Y\}$ in Appendix A, the expectation of (28) is

$$\mathbb{E}\{T_2\} = \beta_d^{3/2} \sqrt{\beta_{br}\beta_{ru}} NB\pi, \quad (30)$$

where $B = MA + \mathbf{a}_b^H \mathbf{R}_d^2 \mathbf{a}_b / 2A$.

Term 3: The expectation of term 3 is,

$$\mathbb{E}\{T_3\} = 2\beta_d \beta_{br} \beta_{ru} M \mathbb{E}\{Y^2\} \mathbb{E} \left\{ \mathbf{u}_d^H \mathbf{R}_d \mathbf{u}_d \right\} \\ = 2\beta_d \beta_{br} \beta_{ru} M^2 (N + F), \quad (31)$$

where $\mathbb{E}\{Y^2\}$ is computed in Appendix A.

Term 4: The expectation of term 4 is,

$$\begin{aligned}\mathbb{E}\{T_4\} &= 4\beta_d\beta_{br}\beta_{ru}\mathbb{E}\{Y^2\}\mathbb{E}\left\{\left|\mathbf{a}_b^H\mathbf{R}_d^{1/2}\mathbf{u}_d\right|^2\right\} \\ &= 4\beta_d\beta_{br}\beta_{ru}(N+F)\left\|\mathbf{R}_d^{1/2}\mathbf{a}_b\right\|_2^2,\end{aligned}\quad (32)$$

where $\mathbb{E}\{Y^2\}$ and $\mathbb{E}\left\{\left|\mathbf{a}_b^H\mathbf{R}_d^{1/2}\mathbf{u}_d\right|^2\right\}$ are in Appendix A.

Term 5: Expanding term 5,

$$T_5 = 4M\sqrt{\beta_d}(\beta_{br}\beta_{ru})^{3/2}Y^3\left|\mathbf{a}_b^H\mathbf{R}_d^{1/2}\mathbf{u}_d\right|.$$

The variable Y^3 is a sum of products of the magnitudes of three correlated complex Gaussian random variables. To the best of our knowledge the mean of such terms is intractable without the use of multiple summations and special functions. As such we will use an approximation based on the gamma distribution to approximate the expectation (see Appendix C). Substituting this approximation and the result for $\mathbb{E}\left\{\left|\mathbf{a}_b^H\mathbf{R}_d^{1/2}\mathbf{u}_d\right|\right\}$ from Appendix A, we have,

$$\mathbb{E}\{T_5\} \approx 2M\sqrt{\pi}\sqrt{\beta_d}(\beta_{br}\beta_{ru})^{3/2}\left\|\mathbf{R}_d^{1/2}\mathbf{a}_b\right\|_2 C_1, \quad (33)$$

with $C_1 = b^3a\prod_{k=1}^2(k+a)$ where a and b are defined in Appendix C.

Term 6: Expanding term 6,

$$T_6 = (M\beta_{br}\beta_{ru})^2 Y^4.$$

Since Y^4 is even more complex than Y^3 we re-use the gamma approximation for Y to make progress. Using the approximation for $\mathbb{E}\{Y^4\}$ in Appendix C gives,

$$\mathbb{E}\{T_6\} \approx (M\beta_{br}\beta_{ru})^2 C_2, \quad (34)$$

with $C_2 = b^4a\prod_{k=1}^3(k+a)$ where a and b are defined in Appendix C.

Using (27), (30), (31), (32), (33) and (34) for $\mathbb{E}\{\text{SNR}^2\}$ and subtracting $\mathbb{E}\{\text{SNR}\}^2$ completes the derivation after some algebraic simplification.

APPENDIX C

APPROXIMATIONS FOR $\mathbb{E}\{Y^3\}$ AND $\mathbb{E}\{Y^4\}$

Due to Y being positive and unimodal, and the sum of N random variables, we propose approximations for $\mathbb{E}\{Y^3\}$ and $\mathbb{E}\{Y^4\}$ using a gamma distribution as an approximation for Y ¹. From Appendix A, we know that $\mathbb{E}\{Y\} = N\sqrt{\pi}/2$ and $\mathbb{E}\{Y^2\} = N + F$, where F is defined by (9). Then, the variance of Y is $\text{Var}\{Y\} = N + F - \frac{N^2\pi}{4}$. Using the method of moments, the parameters that define a gamma distribution fit for Y are,

$$\begin{aligned}a &= \frac{\mathbb{E}\{Y\}^2}{\text{Var}\{Y\}} = \frac{N^2\pi}{4(N+F) - N^2\pi}, \\ b &= \frac{\text{Var}\{Y\}}{\mathbb{E}\{Y\}} = \frac{2}{N\sqrt{\pi}}\left(N + F - \frac{N^2\pi}{4}\right),\end{aligned}$$

¹The motivation here is the same used in Sec. V-A where a gamma approximation is used for the SNR.

where a and b are the shape and scale parameters respectively. Suppose $X \sim \mathcal{G}(a, b)$, then the 3rd and 4th moments are

$$\mathbb{E}\{X^3\} = b^3a\prod_{k=1}^2(k+a), \quad \mathbb{E}\{X^4\} = b^4a\prod_{k=1}^3(k+a).$$

Substituting a and b into the above moments yields the results for C_1, C_2 in Sec. III-A.

REFERENCES

- [1] K. Ying *et al.*, "GMD-based hybrid beamforming for large reconfigurable intelligent surface assisted millimeter-wave massive MIMO," *IEEE Access*, vol. 8, pp. 19 530–19 539, 2020.
- [2] Ö. Özdoğan *et al.*, "Using intelligent reflecting surfaces for rank improvement in MIMO communications," in *Proc. IEEE ICCASP*, 2020, pp. 9160–9164.
- [3] Q. Nadeem *et al.*, "Asymptotic max-min SINR analysis of reconfigurable intelligent surface assisted MISO systems," *IEEE Trans. Wireless Commun.*, pp. 1–1, 2020.
- [4] Q. Wu and R. Zhang, "Intelligent reflecting surface enhanced wireless network via joint active and passive beamforming," *IEEE Trans. Wireless Commun.*, vol. 18, no. 11, pp. 5394–5409, 2019.
- [5] H. Yu *et al.*, "Joint design of reconfigurable intelligent surfaces and transmit beamforming under proper and improper Gaussian signaling," *IEEE J. Sel. Areas Commun.*, pp. 1–1, 2020.
- [6] G. Yu *et al.*, "Design, analysis and optimization of a large intelligent reflecting surface aided B5G cellular internet of things," *IEEE Internet Things J.*, pp. 1–1, 2020.
- [7] Q. Nadeem *et al.*, "Intelligent reflecting surface-assisted multi-user MISO communication: Channel estimation and beamforming design," *IEEE Open J. of the Commun. Soc.*, vol. 1, pp. 661–680, 2020.
- [8] J. Zhang *et al.*, "Transmitter design for large intelligent surface-assisted MIMO wireless communication with statistical CSI," in *Proc. IEEE ICC Workshops*, 2020, pp. 1–5.
- [9] J. Dang *et al.*, "Joint beamforming for intelligent reflecting surface aided wireless communication using statistical CSI," *China Communications*, vol. 17, no. 8, pp. 147–157, 2020.
- [10] Q. Nadeem *et al.*, "Opportunistic beamforming using an intelligent reflecting surface without instantaneous CSI," *IEEE Wireless Commun. Lett.*, pp. 1–1, 2020.
- [11] M. M. Zhao *et al.*, "Intelligent reflecting surface enhanced wireless network: Two-timescale beamforming optimization," *IEEE Trans. Wireless Commun.*, pp. 1–1, 2020.
- [12] N. N. Kundu and M. R. McKay, "RIS-Assisted MISO Communication: Optimal Beamformers and Performance Analysis," *arXiv preprint arXiv:2007.08309v1*, 2020. [Online]. Available: <https://arxiv.org/abs/2007.08309v1>
- [13] A. A. Boulogeorgos and A. Alexiou, "Performance analysis of reconfigurable intelligent surface-assisted wireless systems and comparison with relaying," *IEEE Access*, vol. 8, pp. 94 463–94 483, 2020.
- [14] Q. Tao *et al.*, "Performance analysis of intelligent reflecting surface aided communication systems," *IEEE Commun. Lett.*, pp. 1–1, 2020.
- [15] M. Jung *et al.*, "Asymptotic optimality of reconfigurable intelligent surfaces: Passive beamforming and achievable rate," in *Proc. IEEE ICC*, 2020, pp. 1–6.
- [16] M. Abramowitz and I. A. Stegun, *Handbook of Mathematical Functions with Formulas, Graphs, and Mathematical Tables*. Dover, 1964.
- [17] C. L. Miller *et al.*, "Analytical framework for full-dimensional massive MIMO with ray-based channels," *IEEE J. Sel. Topics Signal Process.*, vol. 13, no. 5, pp. 1181–1195, 2019.
- [18] S. Atapattu *et al.*, "A mixture Gamma distribution to model the SNR of wireless channels," *IEEE Trans. Wireless Commun.*, vol. 10, no. 12, pp. 4193–4203, 2011.
- [19] S. Li *et al.*, "Analysis of analog and digital MRC for distributed and centralized MU-MIMO systems," *IEEE Trans. Veh. Technol.*, vol. 68, no. 2, pp. 1948–1952, 2019.
- [20] H. Tataria *et al.*, "Spatial correlation variability in multiuser systems," in *Proc. IEEE ICC*, 2018, pp. 1–7.